

Supplementary Materials for HINTED

Qiming Xia¹ Wei Ye¹ Hai Wu¹ Shijia Zhao¹ Leyuan Xing¹
Xun Huang¹ Jinhao Deng¹ Xin Li² Chenglu Wen^{1*} Cheng Wang¹

¹Fujian Key Laboratory of Sensing and Computing for Smart Cities, Xiamen University, Xiamen, China

²Section of Visual Computing and Interactive Media, Texas A&M University, Texas, USA

1. Evaluation on more datasets.

Besides the KITTI dataset evaluated in our paper, we’ve added experiments on the challenging nuScenes dataset. As shown in Table 1, our HINTED demonstrates significant advantages compared to the previous SOTA method CoIn.

| Data | Method | mAP | NDS |
|------------------------------|-------------|-------|-------|
| nuScenes Sparsely-supervised | CenterPoint | 8.09 | 25.77 |
| | CoIn | 12.47 | 33.79 |
| | Ours | 23.91 | 45.76 |

Table 1. The performance of HINTED on nuScenes dataset.

2. Discussing other density-related algorithms.

We have added a comparison with other density-related methods. As the results shown in Table 2, compared with previous methods, we took into account the relationship between the distribution of hard instances and distance in sparse settings. The designed MDS module is more suitable for detecting hard instances under sparse supervision. As a result, our approach achieves the best performance.

| Cost | Method | Car-3D | | | Car-BEV | | |
|------|----------|-------------|-------------|-------------|-------------|-------------|-------------|
| | | Easy | Mod. | Hard | Easy | Mod. | Hard |
| 2% | Baseline | 89.5 | 79.2 | 72.3 | 91.7 | 86.3 | 83.5 |
| | DTS | 85.6 | 76.7 | 72.4 | 90.0 | 85.2 | 82.3 |
| | IASSD | 89.7 | 80.1 | 76.9 | 94.6 | 88.7 | 85.8 |
| | Ours | 94.3 | 82.5 | 78.7 | 95.7 | 90.1 | 87.1 |

Table 2. Comparison with other density-related algorithms.

3. Comparison with PV-RCNN on Test Split of KITTI

Previous sparsely-supervised 3D object detection algorithms were only validated on the *val* split. In order to comprehensively assess the performance gap between our method and fully supervised algorithms, apart from validating on the *val* split, we also submitted the results obtained on the *test* split to the KITTI official benchmark

*Corresponding author

leaderboard. Tables 3 and 4 respectively present the comparison of our performance on the *test* split with the fully supervised algorithm PVRCNN for 3D detection and BEV (Bird’s Eye View) detection tasks. From the experimental results obtained on the *test* split, our HINTED achieves over 90% performance compared to the fully supervised algorithms on both crucial detection benchmarks. This proves that our method’s performance on the *test* split aligns consistently with that on the *val* split.

4. The Detail of Fusion Module

Due to space constraints in the main text, a detailed explanation of the fusion process of mixed-density features is provided at this stage. As shown in Figure 1, inspired by SE block [1], we employ an attention mechanism to adaptively fuse features. For input feature map B_1 , we initially down-sample its scale to match B_3 with average pooling. Subsequently, we further down-sample the feature map’s scale to $1 \times 1 \times C$ with global average pooling. Finally, after passing through a fully connected layer and a sigmoid function, we obtain a weight λ_1 . The calculation method for weights $\lambda_2, \lambda_3, \bar{\lambda}_1, \bar{\lambda}_2$ and $\bar{\lambda}_3$ follows a similar process as described above. The final mixed feature is obtained by combining these adaptive weights with the features.

5. More results

As shown in the Table 5, we present the results of the HINTED model for all evaluation metrics on the validation set in this section.

References

- [1] Jie Hu, Li Shen, and Gang Sun. Squeeze-and-excitation networks. In *IEEE Computer Society Conference on Computer Vision and Pattern Recognition (CVPR)*, 2018. 1
- [2] Shaoshuai Shi, Chaoxu Guo, Li Jiang, Zhe Wang, Jianping Shi, Xiaogang Wang, and Hongsheng Li. Pv-rcnn: Point-voxel feature set abstraction for 3d object detection. In *Proceedings of the IEEE conference on Computer Vision and Pattern Recognition (CVPR)*, pages 10526 – 10535, 2020. 2

| Setting | Cost | Method | Car-3D | | | Ped.-3D | | | Cyc.-3D | | |
|---------------------|------|------------|--------|--------|--------|---------|--------|--------|---------|--------|--------|
| | | | Easy | Mod. | Hard | Easy | Mod. | Hard | Easy | Mod. | Hard |
| Fully-supervised | 100% | PV-RCNN[2] | 90.25 | 81.43 | 76.82 | 52.17 | 43.29 | 40.29 | 78.60 | 63.71 | 57.65 |
| Sparsely-supervised | 2% | HINTED# | 84.00 | 74.13 | 67.03 | 47.33 | 37.75 | 34.10 | 76.21 | 63.01 | 55.85 |
| Percent(Avg=91.84%) | | | 93.07% | 91.03% | 87.25% | 90.72% | 87.20% | 84.63% | 96.95 | 98.90% | 96.87% |

Table 3. Comparison with PV-RCNN on KITTI *test* split. The results are validated on 3D-detection benchmark. # indicates that TTA is not used.

| Setting | Cost | Method | Car-BEV | | | Ped.-BEV | | | Cyc.-BEV | | |
|---------------------|------|------------|---------|---------|---------|----------|---------|---------|----------|---------|---------|
| | | | Easy | Mod. | Hard | Easy | Mod. | Hard | Easy | Mod. | Hard |
| Fully-supervised | 100% | PV-RCNN[2] | 94.98 | 90.65 % | 86.14 % | 59.86 % | 50.57 % | 46.74 % | 82.49 % | 68.89 % | 62.41 % |
| Sparsely-supervised | 2% | HINTED | 90.61 % | 86.01 % | 79.29 % | 53.09 % | 41.55 % | 39.18 % | 81.53 % | 67.27 % | 60.88 % |
| Percent(Avg=92.33%) | | | 95.39% | 94.88% | 92.04% | 88.69% | 82.16% | 83.82% | 98.83% | 97.64% | 97.54% |

Table 4. Comparison with PV-RCNN on KITTI *test* split. The results are validated on BEV-detection benchmark. # indicates that TTA is not used.

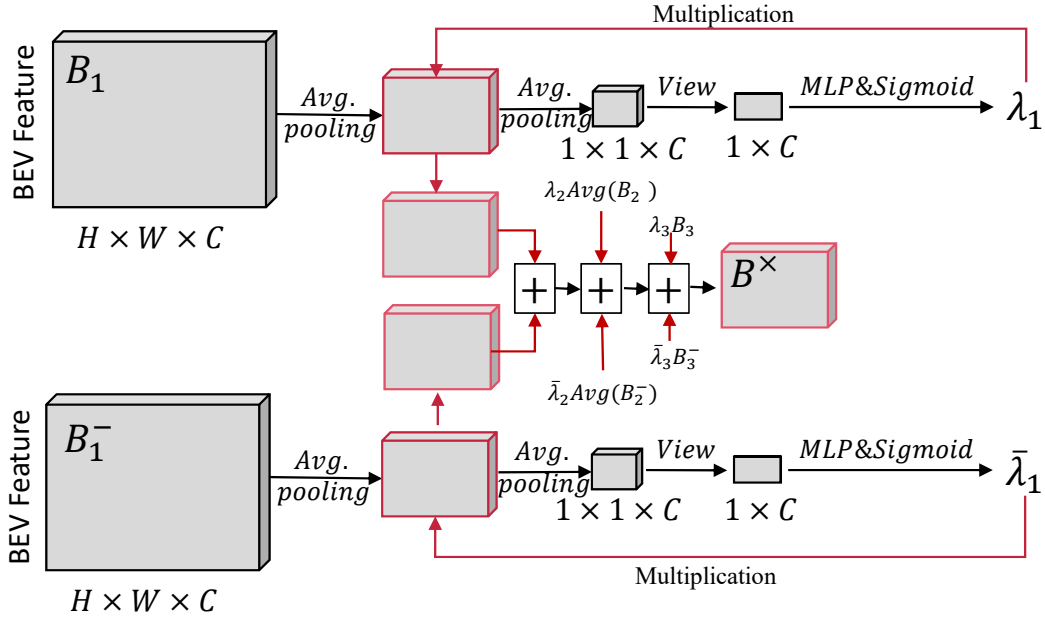


Figure 1. The illustration of fusion module.

| IOU threshold | Metric | Car | | | Ped | | | Cyc | | |
|-----------------|--------|-------|-------|-------|-------|-------|-------|-------|-------|-------|
| | | Easy | Mod | Hard | Easy | Mod | Hard | Easy | Mod | Hard |
| 0.7, 0.5, 0.5 | Bbox | 98.74 | 91.76 | 88.78 | 74.50 | 68.43 | 62.24 | 96.35 | 82.22 | 79.31 |
| | Bev | 95.79 | 90.18 | 87.16 | 69.69 | 63.02 | 56.82 | 95.21 | 78.39 | 73.77 |
| | 3D | 94.33 | 82.56 | 78.75 | 66.53 | 59.97 | 53.77 | 94.69 | 76.37 | 73.05 |
| | Aos | 98.20 | 90.99 | 87.85 | 70.35 | 63.80 | 57.91 | 96.17 | 81.44 | 78.51 |
| 0.5, 0.25, 0.25 | Bbox | 98.74 | 91.76 | 88.78 | 74.50 | 68.43 | 62.24 | 96.35 | 82.22 | 79.31 |
| | Bev | 98.70 | 93.41 | 90.86 | 79.68 | 72.95 | 66.63 | 95.23 | 78.51 | 75.25 |
| | 3D | 98.59 | 91.91 | 90.50 | 79.49 | 72.78 | 66.50 | 95.23 | 78.51 | 75.25 |
| | Aos | 98.20 | 90.99 | 87.85 | 70.35 | 63.80 | 57.91 | 96.17 | 81.44 | 78.51 |

Table 5. Our method's results for all evaluation metrics on the *val* set.